Physics of plasma actuator operating in atmospheric air

Kunwar Pal Singh and Subrata Roy[a)]
Computational Plasma Dynamics Laboratory and Test Facility, Mechanical and Aerospace Engineering, University of Florida, Gainesville, Florida 32611-6300, USA

(Received 25 January 2008; accepted 18 February 2008; published online 19 March 2008)

The physics of plasma actuator operating in the atmospheric air has been numerically investigated. The O^-, O_2^-, O_2^+, and N_2^+ ions have been included in the air chemistry to identify their role. For the specific case study, we find the density of positive ions is an order of magnitude higher at the positive peak of the cycle than that at the negative peak of the cycle. This difference in density levels of the species causes the development of the directional bias of the electrodynamic force. Numerical simulations indicate that positive ions play major role in the development of the positive force.
© *2008 American Institute of Physics*. [DOI: 10.1063/1.2896647]

Electrodynamic modifications of air flowing around flat plates and air craft wings have been investigated both experimentally and numerically.[1–5] These results show that the electrodynamic body force increases with frequency and applied voltage. Specific modality of discharge whether it is glow, Townsend, or streamers will help determine how the body force is transported from charge to neutral species.[6] The effect of this body force in controlling three dimensional laminar and transitional flow structures have been studied utilizing both phenomenological[7] and first-principles plasma kinetics.[3,8]

Recent development of a loosely coupled fluid plasma formulation[9] has shown reasonable success in describing radio frequency (rf) powered electrohydrodynamic control of NACA wing stall, laminar separation over a ramp, boundary layer transition on a flat plate, and turbulent separation over a wall-mounted hump. Unsteady flow actuation with a duty factor seemed to perform better than continuous operation of the rf plasma actuator. These results underscore the importance of accurately resolving the unsteady body force and understanding its transition and turbulence enhancement mechanisms for effective plasma actuation.

Numerical simulations of an asymmetrically arranged dielectric barrier discharge actuator employing multispecies hydrodynamics[5] and Monte Carlo (particle-in-cell and direct simulation Monte Carlo) methods[10] by independent research groups have found that ionization is not equal during positive and negative part of the alternating cycle producing a net force in one direction. Recently, the dc corona discharges and ac dielectric barrier discharges have been investigated under a range of operating conditions. Adjustment of the actuator geometry, dielectric materials, power frequency, and rms voltage show improvement in power transferred to the neutral gas flow by ion-neutral collisions. Also, power losses due to inadequate impedance matching of the power supply to the actuator, dielectric heating, and power required to maintain the atmospheric pressure plasma have been reduced for better performance of the actuator.[4]

In our recent work, we have not included O_2^- in the air chemistry model. In this letter, we investigate physics of plasma operating in air by including O_2^- in the air chemistry. We find that positive ions play an important role in the development of positive electrodynamic force over the flat plat.

Schematic of an asymmetric single dielectric barrier plasma actuator, initial condition, and boundary conditions are same as those reported in Ref. 11. The powered electrode extends from $x=1.7$ cm to $x=1.9$ cm at $y=0.1$ cm; the grounded electrode is from 2.1 to 2.3 cm for the results of Figs. 1–4. An alternating voltage of $\phi = 1000 \sin(10\,000\pi t)$ V is applied to the exposed electrode.

For the air chemistry, we neglect the metastable species along with N^{4+} and O^{4+} due to their extremely high recombination rates. Also, the numerical complexity is further simplified by excluding nitrous oxide at this stage. The model equations governing chemistry of discharge are taken from Ref. 11. We have used chemistry of O_2^- using dissociative

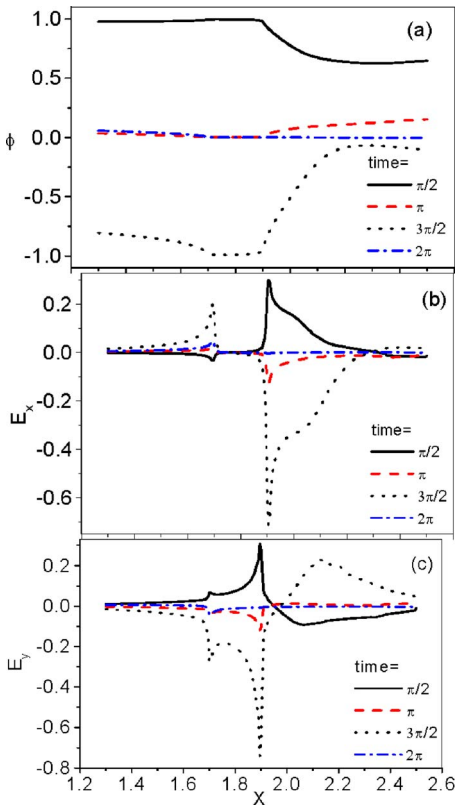

FIG. 1. (Color online) (a) Potential; electric field components (b) E_x and (c) E_y as a function of x at different time points. Here, x is in cm, potential in kV, and electric field in MV m^{-1}.

[a)]Electronic mail: roy@ufl.edu.

 © 2008 American Institute of Physics
Downloaded 19 Mar 2008 to 128.227.50.62. Redistribution subject to AIP license or copyright; see http://apl.aip.org/apl/copyright.jsp

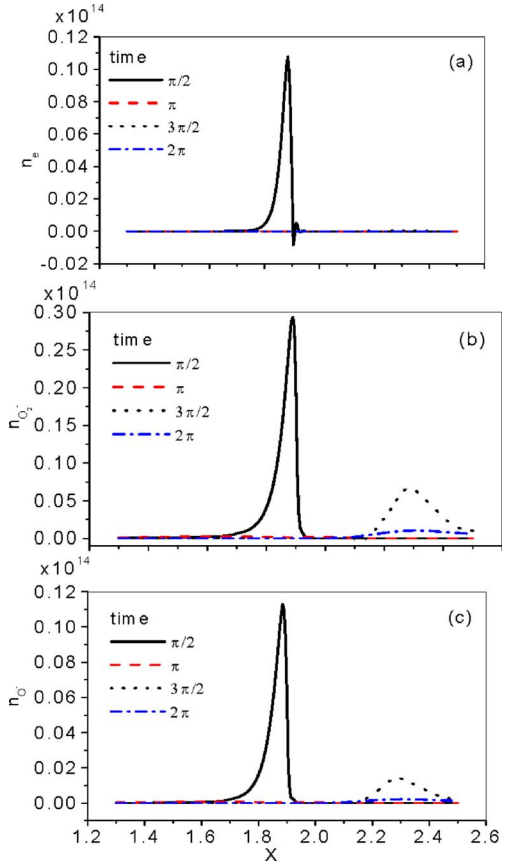

FIG. 2. (Color online) (a) Electron density, (b) density of O_2^-, and (c) density of O^- as a function of x at different time points. Here, x is in cm and density in m^{-3}.

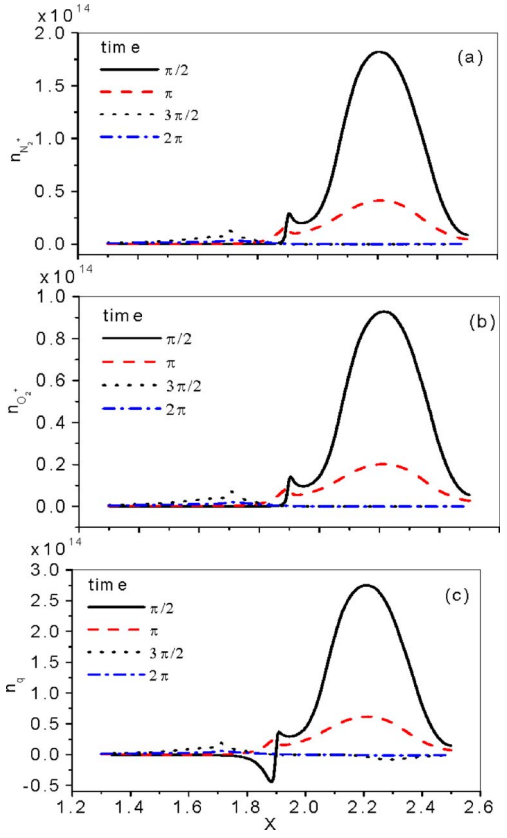

FIG. 3. (Color online) (a) Density of N_2^+, (b) density of O_2^+, and (c) density of charge separation as a function of x at different time points. Here, x is in cm and density in m^{-3}.

attachment and recombination equations $O^- + O_2 \rightarrow O + O_2^-$ and $O_2^- + O_2^+ \rightarrow 2O_2$. The drift-diffusion form of continuity equations with momentum flux $n_\alpha \mathbf{v}_\alpha = -\mathrm{sgn}(e) n_\alpha \mu_\alpha \nabla \phi - D_\alpha \nabla n_\alpha$ for the electrons, ions, and neutrals have been solved with Poisson's equation $\nabla(\varepsilon \nabla \phi) = e(n_e + n_{O^-} + n_{O_2^-} - n_{n_2^+} - n_{O_2^+}) = q$. Various rate coefficients were obtained from Kossyi *et al.*[12] The secondary electron emission from the exposed surface is taken as a function of incident electron energy[13] and remains small, i.e., less than 10^{-3}. No material sputtering of the surface is considered. The mobilities μ_α and diffusion rates D_α are taken from Ellis *et al.*[14] The self-consistent formulation is solved using a Galerkin variational formulation based finite-element method. The details of the numerical procedures are given in our earlier work.[15] Different ion and neutral species are formed as we switch on the rf voltage. Recombination also occurs. The simulation results at $y = 1.05$ mm and for the tenth cycle are given in the following description.

Figure 1(a) shows potential as a function of x at different time points. At positive peak of the cycle, the value of potential is close to the applied rf potential up to the tip of the rf electrode ($x = 1.9$ cm). The potential decreases beyond the tip of the rf electrode. At negative peak of the cycle, the value of potential is close to the applied rf potential up to the tip of the rf electrode ($x = 1.9$ cm). The magnitude of potential decreases sharply beyond the tip of the rf electrode. Figures 1(b) and 1(c) show electric field as a function of x at different time points. The peaks of the electric field are close to the tip of the rf electrode.

Figure 2(a) shows electron density as a function of x at different time points. The oxygen ions O^- are produced through ionization of nitrogen and oxygen molecules. The density of electrons is nearly $1.1 \times 10^{13}/m^3$ at the positive peak of the cycle. Figures 2(b) and 2(c) show density of negative oxygen ions O_2^- and O^-, respectively, as a function of x at different time points. The oxygen ions O^- and O_2^- are produced through dissociative attachment of oxygen molecules with electrons and O^-, respectively. The negative oxygen ions O_2^- and O^- are repelled from the area near to grounded electrode and are attracted toward rf electrode dur-

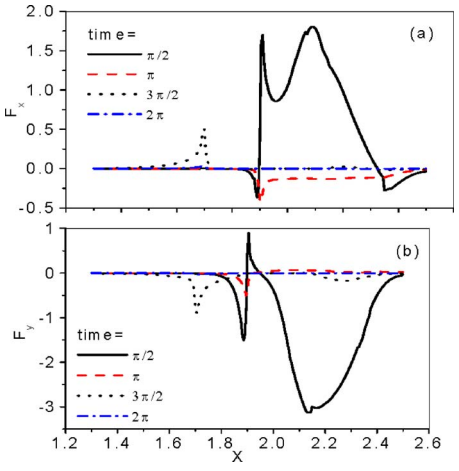

FIG. 4. (Color online) Electrodynamic force components (a) F_x and (b) F_y as a function of x at different time points. Here, x is in cm and force in $N\,m^{-3}$.

Downloaded 19 Mar 2008 to 128.227.50.62. Redistribution subject to AIP license or copyright; see http://apl.aip.org/apl/copyright.jsp

ing positive part of the cycle. The reverse happens during negative part of the cycle. The negative oxygen ions O_2^- and O^- are deposited from $x=2.2$ cm to $x=2.4$ cm over the surface of dielectric. The density of negative oxygen ions is one order of magnitude higher at positive peak of the cycle than that at the negative peak of the cycle. The densities of negative oxygen ions O_2^- and O^- are nearly $3\times10^{13}/m^3$ and $1.1\times10^{13}/m^3$ at the positive peak of the cycle. The tip of rf electrode is at $x=1.9$ cm.

Figures 3(a) and 3(b) show the density of nitrogen ions N_2^+ and oxygen ions O_2^+, respectively, as a function of x at different time points. The nitrogen ions N_2^+ and oxygen ions O_2^+ are produced through ionization of nitrogen and oxygen molecules. The positive ions are repelled from the area of rf electrode and are attracted toward grounded electrode during positive part of the cycle. The maximum density of nitrogen ions N_2^+ and oxygen ions O_2^+ are nearly $1.75\times10^{14}/m^3$ and $9\times10^{13}/m^3$, respectively, at the positive peak of the cycle. The N_2^+ and O_2^+ respond to electric field in a similar manner, hence, their density profiles are similar to each other. The nitrogen and oxygen ions are concentrated in the sheath region from $x=2.1$ to 2.4 cm. The difference between density levels of nitrogen and oxygen is because of the ratio of parent gas molecules in atmospheric air and the difference in their rate coefficients. The motion of charged particles gives rise to charge separation $n_q=n_{O_2^+}+n_{N_2^+}-n_e-n_{O^-}-n_{O_2^-}$. Figure 3(c) shows density of charge separation as a function of x at different time points. It is similar to the density profiles of positive nitrogen and oxygen ions. The densities of negatively charge species are small in comparison to densities of positive species. The value of charge separation $q=en_q$ is nearly equal to the sum of density of nitrogen ions N_2^+ and oxygen ions O_2^+. Charge separation gives rise to a self-generated electric field through Poisson's equation. The densities decrease sharply with the increase in the value of y (not shown).

Figures 4(a) and 4(b) show electrodynamic force components $F_x=qE_x$ and $F_y=qE_y$, respectively, as a function of x at different time points. The maximum F_x force is positive at the positive peak of the cycle and the maximum F_y force is negative at the positive peak of the cycle. Both components of the electrodynamic force F_x and F_y are concentrated from $x=2.0$ to 2.4 cm.

The electrons are repelled from the area close to the grounded electrode and are attracted toward rf electrode during positive part of the cycle where they are lost. When negative part of the cycle starts, there are not plenty of electrons to contribute to ionization process. The electrons are attracted toward grounded electrode during negative part of the cycle and get deposited over the surface of dielectric. When positive part of the cycle starts, there are plenty of electrons to contribute to ionization process. The density of electrons is an order of magnitude higher at positive peak of the cycle than that at the negative peak of the cycle. Such higher concentration contributes greatly in the collisional process and produces high ion density during the positive phase of the cycle. The density of positive ions is an order of magnitude higher at the positive peak of the cycle than that at negative peak of the cycle. The density of positive ions is higher than that of negative ions. This difference in density levels of the species is responsible for the development of the electric force over a flat plate. Our results are similar to that reported by Font *et al.*[10] and can be supported by the experimental findings of Takizawa *et al.*[16]

We have also carried out simulations of a case (not shown) with the powered electrode extending from $x=1.5$ cm to $x=1.9$ cm at $y=0.1$ cm, and the grounded electrode from 2.1 cm to 2.5 cm. We found that the maximum value of the charge separation decreases and the distribution of charge separation becomes wider, extending beyond $x=2.6$ cm. The maximum of the x-component of the force was slightly higher and the profile was wider for this case. The direction of electric field alters with the increase in the length of electrodes which causes above mentioned effects.

In conclusion, the density of positive ions is an order of magnitude higher at the positive peak of the cycle than that at negative peak of the cycle. Based on the reaction rate coefficients used, the density of positive ions is higher than that of the negative ions. This difference in density levels of the species is responsible for the development of the positive electrodynamic force over a flat plate. The positive ions play an important role in the development of the positive force. Such explanation is also reasonable for dc plasma actuators.

This work was partially supported by the AFOSR grant monitored by Dr. John Schmisseur and the Air Force Research Laboratory contract.

[1] C. L. Enloe, T. E. McLaughlin, R. D. Van Dyken, K. D. Kachner, E. J. Jumper, T. C. Corke, M. Post, and O. Haddad, AIAA J. **42**, 595 (2004).
[2] J. R. Roth, Phys. Plasmas **10**, 2117 (2003).
[3] S. Roy, Appl. Phys. Lett. **86**, 101502 (2005).
[4] J. R. Roth and X. Dai, Proceedings of the 44th AIAA Aerospace Sciences Meeting and Exhibit, Reno, Nevada, 9–12 January, 2006 (AIAA, Washington, D.C., 2002), Paper No. AIAA-2006-1203; K. P. Singh and S. Roy, Appl. Phys. Lett. **91**, 081504 (2007).
[5] K. P. Singh, S. Roy, and D. Gaitonde, Plasma Sources Sci. Technol. **15**, 735 (2006).
[6] C. Baird, C. L. Enloe, T. E. McLaughlin, and J. W. Baughn, Proceedings of the 43rd Aerospace Sciences Meeting, Reno, Nevada, 2005 (AIAA, Washington, D.C., 2002), Paper No. AIAA-2005-0565.
[7] W. Shyy, B. Jayaraman, and A. Anderson, J. Appl. Phys. **92**, 6434 (2002).
[8] K. P. Singh and S. Roy, J. Appl. Phys. **98**, 083303 (2005); B. Jayaraman, S. Thakur, and W. Shyy, J. Heat Transfer **129**, 517 (2007); A. V. Likhanskii, M. N. Shneider, S. O. Macheret, and R. B. Miles, Phys. Plasmas **14**, 073501 (2007).
[9] D. Gaitonde, M. Visbal, and S. Roy, ASME Joint U.S.-European Fluids Engineering Summer Meeting, Miami, 2006 (AIAA, Washington, D.C., 2002), Keynote Lecture FEDSM2006-98553; M. Visbal, D. Gaitonde, and S. Roy, Proceedings of the Fluid Dynamics and Flow Control Conference, San Francisco, June 2006 (AIAA, Washington, D.C., 2002), Paper No. AIAA-2006-3230.
[10] G. I. Font, C. L. Enloe, T. E. McLaughlin, and D. Orlov, Proceedings of the 45th Aerospace Sciences Meeting and Exhibit, Reno, Nevada, 2007 (AIAA, Washington, D.C., 2002), Paper No. AIAA-2007-188.
[11] K. P. Singh and S. Roy, J. Appl. Phys. **101**, 123308 (2007).
[12] I. A. Kossyi, A. Yu. Kostinsky, A. A. Matveyev, and V. P. Silakov, Plasma Sources Sci. Technol. **1**, 207 (1992).
[13] S. Roy and B. P. Pandey, Phys. Plasmas **9**, 4052 (2002).
[14] H. W. Ellis, R. Y. Pai, E. W. McDaniel, E. A. Mason, and L. A. Viehland, At. Data Nucl. Data Tables **17**, 177 (1976).
[15] S. Roy and D. Gaitonde, Phys. Plasmas **13**, 023503 (2006).
[16] Y. Takizawa, A. Matsuda, K. Kikuchi, A. Sasoh, and T. Abe, Proceedings of the 38th AIAA Plasma Dynamics and Lasers Conference, June 2007 (AIAA, Washington, D.C., 2002), Paper No. AIAA-2008-4376.

Downloaded 19 Mar 2008 to 128.227.50.62. Redistribution subject to AIP license or copyright; see http://apl.aip.org/apl/copyright.jsp